

IMPREGNATION BEHAVIOR OF CARBON FIBER FABRIC UNDERNEATH THE ROLLERS IN DOUBLE BELT PRESS

Osuke Ishida¹, Junichi Kitada², Katsuhiko Nunotani³ and Kiyoshi Uzawa⁴

¹Innovative Composite Materials Research and Development Center
Kanazawa Institute of Technology, 2-2 Yatsukaho, Hakusan 924-0838, Japan

¹Email: o-ishida@neptune.kanazawa-it.ac.jp,

³Email: nuno@neptune.kanazawa-it.ac.jp,

⁴Email: uzawa@neptune.kanazawa-it.ac.jp,

Web Page: <http://www.icc-kit.jp/>

²PROCESS SYSTEMS K.K., 1-18 Mitsugaoka Nishiku, Kobe 651-2228, Japan

Email: junichi.kitada@ipco.com,

Web Page: <http://www.ipco.com/jp>

Keywords: Thermoplastic composite, Impregnation process, Continuous processing, Double belt press

Abstract

The subject of this study is to investigate thermoplastic impregnation process of carbon fiber fabric under pressure rollers in double belt press. Fixed rollers double belt press is effective for the mass production of thermoplastic composite sheet. The key factor of this system is the appropriate setting of belt gaps under rollers, which determine the pressure made by the balance of out-of-plane impregnation and in-plane resin flow. The resin in-plane flow often cause the fabric distortion.

In this study, an experimental model was developed to investigate these process. The mold was mounted on a testing machine which controls the load or crosshead speed. Carbon fiber woven fabrics and high viscositic liquid resin were stacked in the mold. While the mold was compressed, the material thickness reduction and resulting force was monitored during process. From the results, the impregnation process, permeability and in-plane resin flow was evaluated based on the theory of Darcy's law and plane Poiseuille flow. To understand these mechanism will lead to find the efficient impregnation process with minimizing the rein backflow in double belt press.

1. Introduction

Thermoplastic carbon fiber composite sheet, so-called organosheet, is a promising material for industrial and automobile parts due to the possibility of short cycle production by stamp forming. The key factors for CFRTP production are the impregnation quality and low cost manufacturing process. However, it is difficult to achieve these properties at the same time because the impregnation of carbon fiber fabric with thermoplastic resin is difficult due to resin's high melt viscosity. The process needs long time and much pressure, which makes the production cost much higher.

A double belt press (DBP) machine was used for the production of organosheet. The machine is consisted of heat and pressure zone for impregnation and subsequent cooling zone for consolidation, which enables the continuous production process. For the efficient production the process parameters should be optimized based on the understanding of the process mechanism. Several investigations have been reported about the process of DBP so far [1-3]. Fixed rollers DBP has several fixed rollers in the heating zone where the minimum gaps between the vertical rollers can be controlled. This

system allows the possibilities for discontinuous fiber fabrics or thick materials that have a difficulty in keeping the thickness using a hydraulic press. However, this mechanism is more complicated than hydraulic pressure system. Under the rollers both of out-of-plane impregnation and in-plane resin flow occur and the resulting pressure is defined by these combination.

In our previous study, the impregnation process model of fixed rollers DBP was developed [4]. But the detailed behavior underneath rollers couldn't be analyzed. In this study the experimental model was developed to investigate the impregnation and resin in-plane flow under rollers using a testing machine. The result was evaluated and compared with the theory based on Darcy's law and plane Poiseuille flow.

2. Double belt press

The image of double belt press is shown in Fig.1. In the heating zones, 8 rollers are installed in the one housing. The vertical positions of rollers are fixed in the machine to keep the target belt gaps. While the material thickness reduce under rollers, out-of-plane impregnation and in-plane resin flow occur with fabric compaction. The resulting pressure is balanced by these flows. The process is illustrated in Fig.2. In order to obtain the efficient impregnation process, it's important to understand these mechanism.

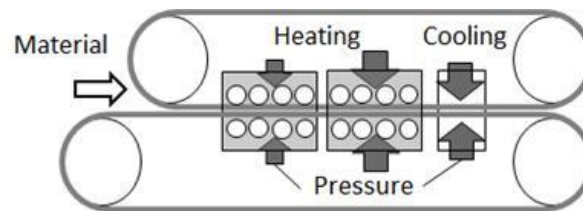


Fig. 1 Schematic view of double belt press

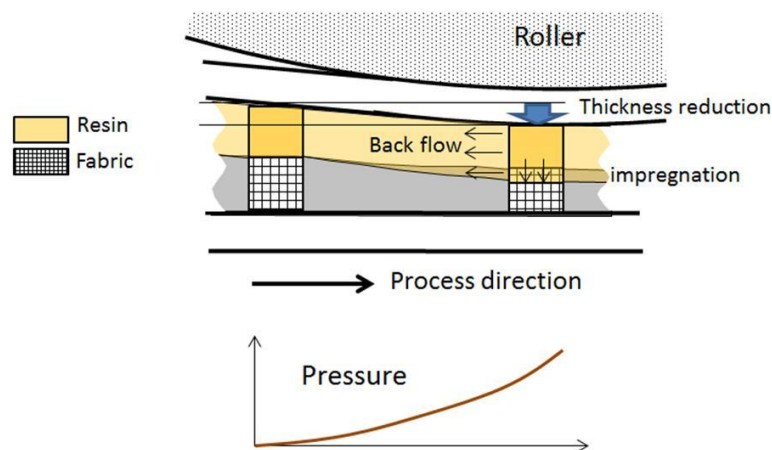


Fig. 2 Impregnation and pressure behavior under roller

3. Experimentals

3.1. Materials

Carbon fiber plain woven fabric (T700SC-12K, 3.27yarns/25mm, 210g/m², Toray co., ltd.) and standard liquid resin for calibrating viscometers (JS160000, 151.5mPa·s at 20°C, Nippon Grease Co., Ltd.) were used. The fabric was cut to the size of 40mm x 40mm, and the resin was applied on both surfaces with the equivalent thickness of 50 μm. 5ply of the fabrics were layed up in the mold.

3.2. Experimental equipment

A metal mold (Cavity size: 40mm x 40mm) was mounted on the fixture that was connected to a load cell (5kN) and a testing machine (AG-Xplus, Shimadzu Co., Ltd.). The mold was available for shear-edge state or open-edge state with/without the attachment of two opposite side walls. This system is illustrated in Fig. 3. Tensile force of the testing machine makes compression force on the material in the mold. The cross-head movement and the force detected by load cell were recorded at the time step of 0.1s. The fixture was slightly deformed by the applied force. This deformation had a non-negligible effect due to the small material thickness reduction. Therefore, the deformation amount from blank test was subtracted from the measured data at each step of the force.

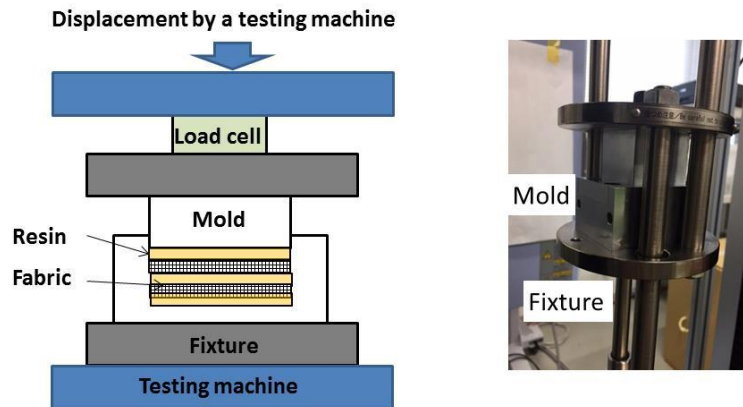


Fig. 3. Experimental equipment for impregnation process model

3.3. Test process conditions

Three kinds of experiments were conducted to evaluate the impregnation and resin flow at the room temperature. The first test was performed using the lay-up of resin and fabrics with the shear-edge mold in order to evaluate impregnation. The second test was performed using resin only with the open-edge mold in order to evaluate resin in-plane flow. And the third test was performed using the lay-up of resin and fabrics with the open-edge mold in order to evaluate the combination behavior of impregnation and resin in-plane flow. The movement of the fixture was controlled by a constant load or given cross-head speed of the testing machine. The test conditions were summarized in Table. 1.

Table.1. Test process conditions

<i>Evaluated process</i>	<i>Material</i>	<i>Mold type</i>	<i>Fixture movement controll</i>
Impregnation	Resin and fabrics	Shear-edge	Constant load (640N, 1280N) or cross-head speed (0.5mm/min, 1mm/min)
Resin flow	Resin	Open-edge	Cross-head speed (0.5mm/min, 1mm/min)
Impregnation and resin flow	Resin and fabrics	Open-edge	Constant load (640N, 1280N)

Before these experiments, the compaction behavior of 5ply of dry fabrics was measured at a cross-head speed of 0.5mm/min. The pressure and v_f were calculated from the position and force of the machine. v_f was defined as the fabric volume divided by the mold volume. The mean value of five measurements was obtained.

4. Results and discussions

4.1. Analysis of impregnation process model

In the first step, the compaction behavior of the fabric is shown in Fig. 4. The relationship between pressure and v_f could be fitted with the power law as the following equation.

$$v_f = 0.560P^{0.050} \quad (1)$$

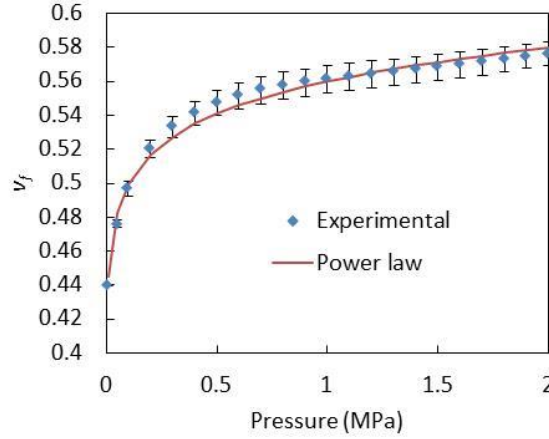


Fig. 4 Fabric compaction behavior

Figure 5 shows the experimental results of impregnation process model. Mold gap indicates the material thickness after the upper mold contacted the material surface.

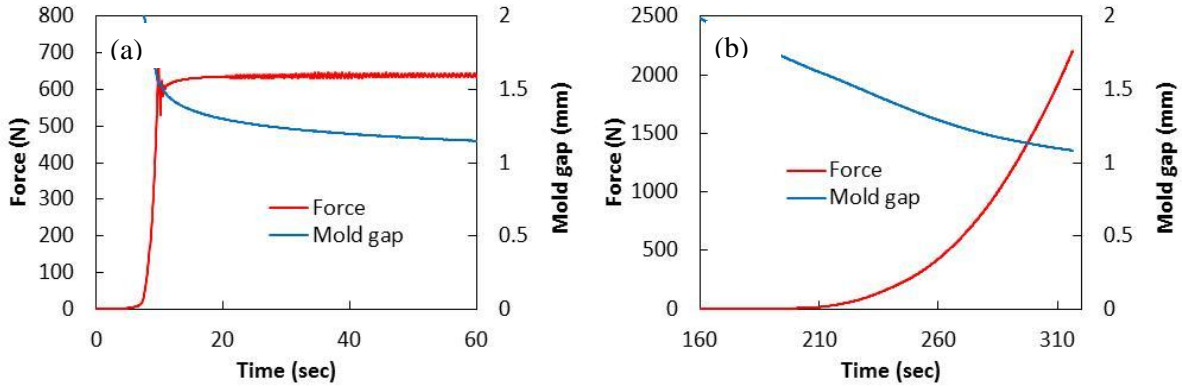


Fig. 5 Experimental results of impregnation model: (a) load control of 640N, (b) cross-head speed control of 0.5mm/min

In several papers, the impregnation process model was investigated according to the configuration of fiber bundles in the fabric[5-7]. However, it seems difficult to define the bundle shape in the woven fabric in this experiment. Therefore, simple impregnation model was developed for the fabric scale. At first, the material thickness reduction involves not only the impregnation but also the fabric compaction. Especially in the case of pressure-shifting with time as shown in Fig. 5(b), the fabric compaction would increase with the pressure increase. In order to calculate the impregnation flow from the material thickness reduction, the mass balance inside the mold cavity was calculated at each time step taking into account the fabric compaction as described in Eq. (1). In this equation, the fabric compaction was assumed to occur only in the un-impregnated area of the fabric.

$$\frac{V_{fab} - V_{fab}^i}{v_f} + V_{fab}^i + V_{res} = V_{mold} \quad (2)$$

$$V_{fab}^i = \frac{V_{fab} + v_f(V_{res} - V_{mold})}{(1 - v_f)} \quad (3)$$

where V_{fab} is the volume of fabric, V_{fab}^i is the impregnated volume of fabric, V_{res} is the volume of resin and V_{mold} is the volume of the mold cavity. It's noted that the fiber bundles configuration in the fabric was ignored and assumed to be uniform in this calculation. The equation will lead to the impregnation length and impregnation flow rate.

$$L = \sum \Delta L = \sum \frac{V_{fab}^i}{Av_f} \quad (4)$$

$$\frac{Q_1}{A} = \Delta L(1 - v_f) \quad (5)$$

where L is the impregnation length, ΔL is the difference of L at each time step, Q_1 is the impregnation flow rate and A is the area of base.

The permeability was calculated at each time step based on Darcy's law with one direction flow using the parameter value from Eq. (1)–(5).

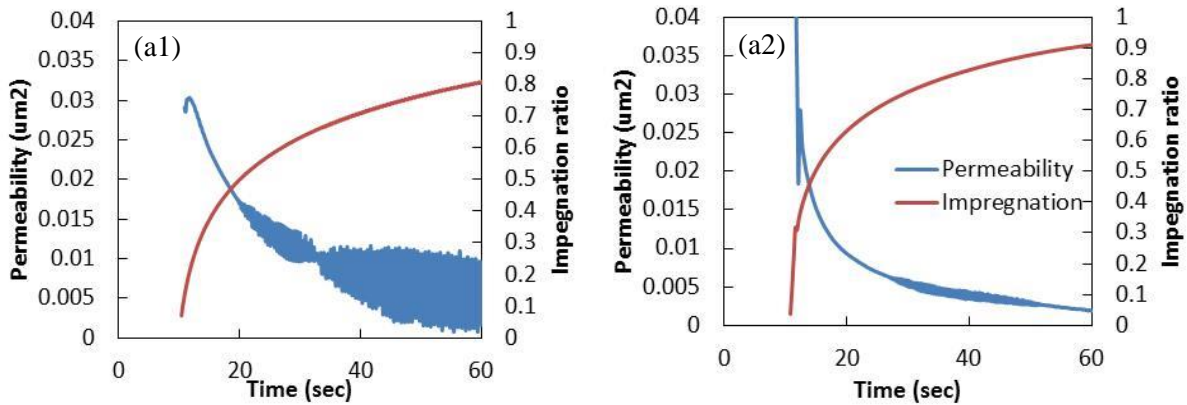
$$K = \frac{Q_1 \mu L}{A P} \quad (6)$$

where K is the permeability, μ is the resin viscosity and P is the pressure.

The v_{fi} in the impregnated area of fabric was calculated as following.

$$v_{fi} = \frac{V_{fab}^i}{AL} \quad (7)$$

The calculated permeabilities and impregnation rates are shown in Fig. 6. The permeability decreased with the impregnation progress at every test condition. It's probably because the configuration of fiber bundles is ignored in these calculation and the resin start to percolate preferably into the low density area such as outside bundles or disordered area of the bundles surface, subsequently go to the saturation of bundle dense core. In the case of higher pressure condition, the overall permeability curve was lower because the v_{fi} was higher. From these results, the permeabilities were summarized and re-plotted as a function of the impregnation ratio multiplying v_{fi} as shown in Fig. 7. The curves were almost similar with every test condition and it suggests that this model can predict the permeability curve to some degree from the impregnation ratio and v_{fi} .



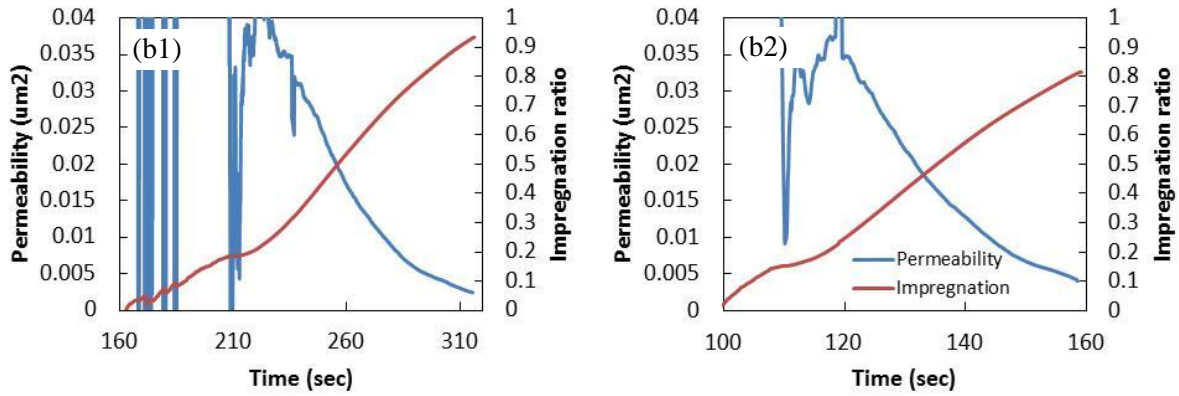


Fig. 6. Permeability and impregnation ratio: (a1) load control of 640N, (a2) load control of 1280N, (b1) cross-head speed control of 0.5mm/min, (b2) cross-head speed control of 1mm/min

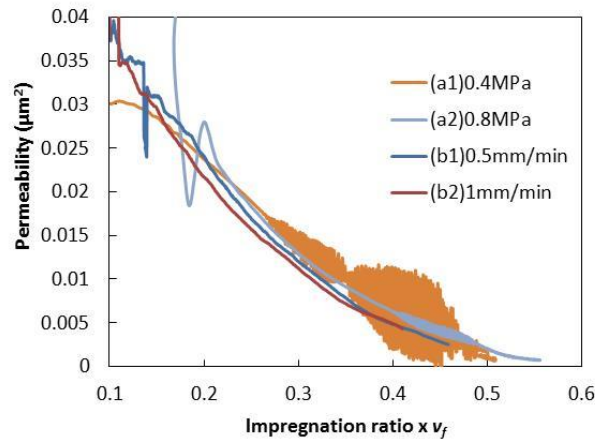


Fig. 7 Relationship between permeability and impregnation ratio multiplied by v_f

4.2. Analysis of resin flow process model

The resin in-plane flow was assumed as the pressure-driven Poiseuille flow between two plates. In this experiment, two opposite side edges of the mold were open, which allowed the resin outflow with two directions. The flow rate could be shown in the following equation.

$$Q_2 = \frac{h^3 w}{12\mu} \frac{dP_i}{dl} \quad (8)$$

where Q_2 is resin in-plane flow, h is the thickness of resin, w is the width of flow, dp_i/dl is the pressure gradient of the flow direction. As the upper plate moves down with the speed of u , Q_2 was also expressed as following equation at the distance of l from the center in the mold.

$$Q_2 = wlu \quad (9)$$

where u is the speed of the resin thickness reduction. Substituting Eq. (8) in (9) and intergrating from the flow position of 0 to l results in

$$\Delta P_i(l) = \frac{6\mu l^2 u}{h^3} \quad (10)$$

where $\Delta P_i(l)$ is the pressure difference from the center to the distance of l from it.

At the open edges in the mold the pressure equals to the atmospheric pressure, therefore, the total applied force can be calculated as the intergration on the surface as shown in the following equation.

$$F = 2w \int_0^{l_e} \left(\frac{6\mu l_e^2 u}{h^3} - \frac{6\mu l^2 u}{h^3} \right) dl = \frac{8w\mu l_e^3 u}{h^3} \quad (11)$$

where l_e is the distance from the center to the edge in the mold. From Eq. (11), the force profile over the process time could be calculated.

Fig. 8 shows the force curves at the test conditions of cross-head speed of 0.5mm/min and 1mm/min. The graphs also show the theoretical curves calculated from Eq. (11). They show some discrepancy especially in the initial stage, however, the model was reasonable enough to evaluate the effect of process parameters.

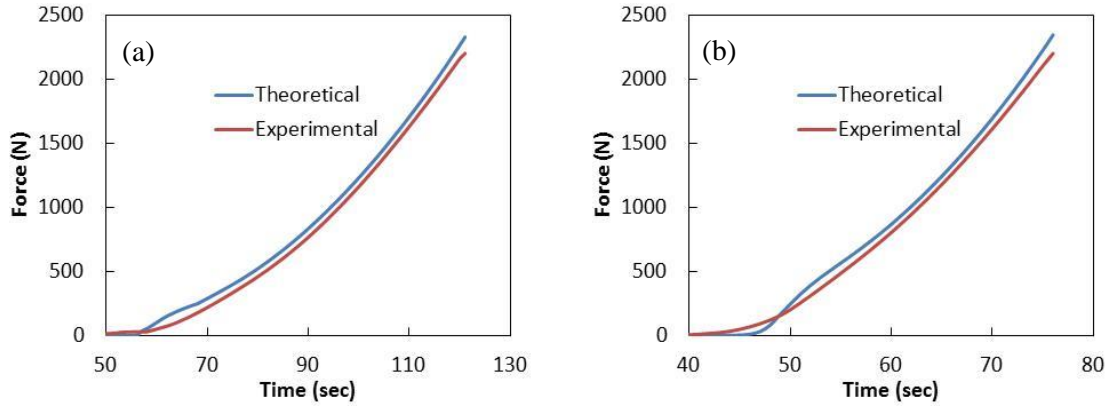


Fig. 8 The comparison of experimental and theoretical force curves in in-plane resin flow: (a) cross-head speed of 0.5mm/min, (b) cross-head speed of 1mm/min

4.3. Analysis of the combination of impregnation and resin flow process model

As described in Fig.2, out-of-plane impregnation and resin in-plane flow was caused by the pressure gradient while the material was compressed. The theoretical process model could be described by the combination of Eq. (1)-(6) for impregnation and Eq. (8) for resin in-plane flow in a resin layer. Thickness variation in a resin layer has a strong influence on the in-plane flow rate as expected from the equation. Furthermore, resin layer thickness decrease with the progress of impregnation and resin in-plane flow. Here the resin in-lane flow inside the fabric was ignored for simplicity, and the resin layer thickness at the time t could be roughly assumed as following equation.

$$h(t) = h_o - \int_0^t \frac{Q_1}{A} dt - \int_0^t \frac{Q_2}{A} dt \quad (12)$$

where h_o is the original resin thickness.

The experiments were performed with the load control of 640N and 1280N for 60s. The two type of resin thickness of 50 μ m and 65 μ m were also evaluated with the load control of 640N. At the end of process, the resin outflow was scraped up and the amount was measured. And the impregnation ratio was calculated based on Eq. (3) with subtracting the outflow amount. Table. 2 shows the summary of impregnation ratio and the amount of resin outflow at the end of process.

Table. 2 Summary of the combination of impregnation and resin flow process

Process condition	Impregnation ratio	weight of resin outflow
Load control of 640N and resin thickness of 50 μ m	0.79	0.07g
Load control of 640N and resin thickness of 65 μ m	0.84	0.14g
Load control of 1280N and resin thickness of 50 μ m	0.92	0.09g

The final impregnation ratio in these experiments were close to the value obtained from the experiments with shear-edge mold as described in Section 4.1. It's probably because the pressure and the holding time was the same. On the other hand, the resin outflow was different at each test condition. When the applied load was higher, the outflow was bigger. Furthermore, when the resin thickness was higher, the outflow was much bigger. These results was expected from Eq.(8). The suggested efficient process to get good impregnation and low resin outflow could be described that the low pressure is applied at the early stage of process in order to make the impregnation with higher permeability and minimize resin in-plane flow, and after the resin layer thickness is decreased enough the high pressure can be applied to get the further impregnation.

5. Conclusions

The experimental process model was developed in order to analyze the out-of-plane impregnation and in-plane resin flow with the lay-up material of carbon fiber woven fabric and resin.

From the experiments of out-of-plane impregnation model, the curves of permeability, impregnation ratio and v_f were calculated and these indicated the good relationship based on the theory of Darcy's law. The experimental in-plane resin flow model confirmed the good predictability by the theory of plain Poiseuille flow. Finally, the experimental model of those combination confirmed that the in-plane resin flow was influenced by the pressure and resin layer thickness as expected from the theory. The efficient process with controlling pressure was suggested in order to obtain good impregnation and reduce in-plane resin flow.

In the future study, these process model will be further investigated and applied to the process simulation under rollers in double belt press, which will lead to the base of the parameter optimization.

Acknowledgments

This study was supported by COI program "Construction of Next-generation Infrastructure System Using Innovative Composite Materials: Enabling Society to Coexist with Earth for Centuries in Safety and Security" by JST

References

- [1] X. Wang, C. Mayer and M. Neitzel. Some issues on impregnation in manufacturing of thermoplastic composites by using a double belt press, *Polymer Composites*, 18, 6, 701-710, 1997.
- [2] C. Mayer, X. Wang and M. Neitzel. Macro-and micro-impregnation phenomena in continuous manufacturing of fabric reinforced thermoplastic composites. *Composites Part A*, 29, 783-793, 1998.
- [3] A. Trende, B.T. Astrom, A.Woginger, C. Mayer and M. Neitzel. Modeling of heat transfer in thermoplastic composites manufacturing: double-belt press lamination. *Composites Part A*, 30, 935-943, 1999.
- [4] O. Ishida, G. Fukushima, J. Kiada, T. Sekido and K. Uzawa. Continuous impregnation process by fixed rollers double belt press. *Proceedings of ECCM17*, 2016.
- [5] N. Bernet, V. Michaud, P.-E. Bourban and J.-A.E.Manson. An impregnation model for the consolidation of thermoplastic composites made from commingled yarns. *Journal of Composite Materials*, 33, 8, 751-772, 1999.
- [6] B.P.Van West, R. Byron Pipes, M.keefe and S.G. Advani. The draping and consolidation of commingled fabrics. *Composites Manufacturing*, 2, 1, 10-22, 1991.
- [7] Y. Wang and S.M. Grove. Modelling microscopic flow in woven fabric reinforcements and its application in dual-scale resin infusion modelling. *Composites Part A*, 39, 843-855, 2008.